CHIMIA 48 (1994) Nr. 3 (März)

Chimia 48 (1994) 43–49

ISSN 0009–4293

Photofragment Translational Spectroscopy

Peter Felder*

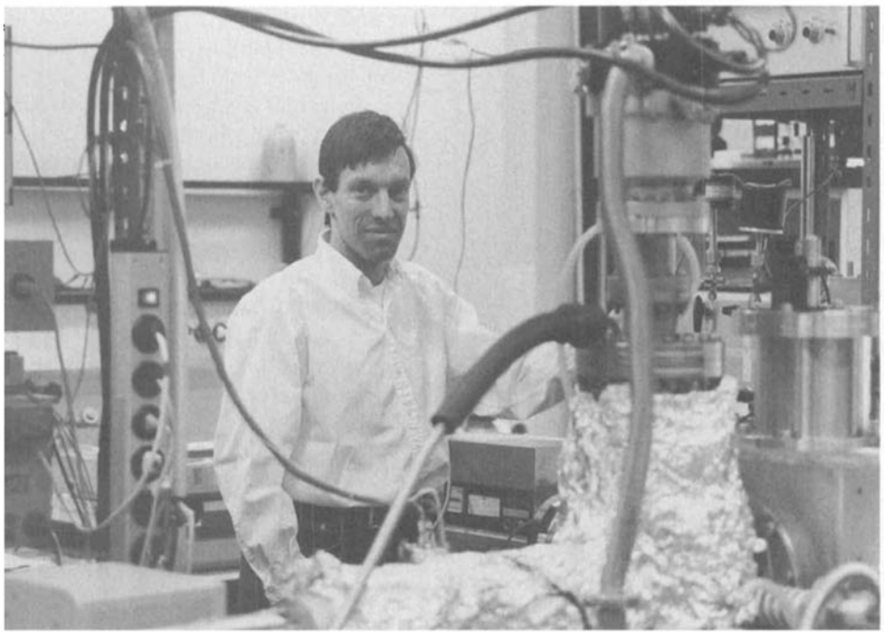

Peter Felder: Born on 27. December 1951 in Milano (Italy). 1974 Diploma in Chemistry at ETH-Zürich. 1981 PhD at ETH-Zürich (Prof. *Hs. H. Günthard*, Molekularstrahlmethoden und Matrixspektroskopie). 1982–1984 Postdoctoral Fellow at the *Lawrence Berkeley* Laboratory of the University of California at Berkeley (USA). Since 1984 Universität Zürich. 1993 Habilitation Universität Zürich (Photofragment Translational Spectroscopy). 1993 *Werner* Medal of the New Swiss Chemical Society.
Research topics: Gas-phase photochemistry and reaction dynamics.
Laser and molecular beam methods in materials research (high-temperature superconductivity).

Abstract. Photofragment translational spectroscopy (PTS) is a technique for studying the mechanisms and the dynamics of photodissociation processes under collision-free conditions. After a brief introduction to the methodology of PTS, a high-performance apparatus developed in our laboratory is described. Various applications are then presented to demonstrate the versatility of this technique. Examples include studies of the photodissociation dynamics of small molecules and the investigation of decomposition mechanisms in atmospherically important molecules.

The photodissociation of molecules in the gas phase is a challenging and rewarding subject. There are three important reasons for this interest. First of all, the dissociation of an isolated molecule in the absence of collisions may be considered as a *prototypical chemical event* [1][2]. Its conceptual simplicity has allowed theoreticians and experimentalists to gain insight into the microscopic dynamics of chemical reactions [3][4]. Second, photodissociation processes are *environmentally important*. Several reactive species formed upon solar irradiation are known to play key roles in the chemistry of our atmosphere [5][6]. Accordingly, the development of reliable atmospheric models [7] requires a thorough understanding of the primary photochemical processes. The third reason for seeking knowledge about photochemistry is the quest for its control. The goal of *selective photochemistry* [8] has been pursued since the advent of powerful laser systems and, indeed, laser-assisted chemistry has been proven useful for the separation of isotopes [9] and for the deposition of thin material layers with novel properties [10].

In general terms, when studying the photodissociation of a polyatomic molecule ABCD, one needs first to establish the occurrence and relative importance of various possible decay modes (*e.g.* the formation of AB + CD as opposed to ABC + D). Having determined the 'chemical identity' of the reaction products, one can proceed to study the dynamics of their formation. This is conveniently done by carrying out a photodissociation experiment under *collisionless conditions*, *i.e.* in a low pressure gas or, even better, in a molecular beam. By probing various properties of the nascent photofragments, it is possible to unravel the details of the microscopic course of the reaction. Among the techniques for 'interrogation' of the reaction products, laser spectroscopic methods [11] can provide a wealth of information including, most notably, the distribution of product quantum states and the so-called vector correlations [12]. Moreover, the development of ultrafast laser pulses has promoted 'real-time' studies of chemical reaction dynamics [13]. Concurrent with their high specificity, however, laser spectroscopic detection methods generally require that the photofragments to be probed have favorable spectroscopic properties, in other words, the spectral positions and inherent intensities of the pertinent transitions should be well known. Accordingly, spectroscopic fragment probing has been most successful for atomic and diatomic species.

Photofragment translational spectroscopy (PTS), which was pioneered by *Wilson* and coworkers[14], is in many respects complementary to optical fragment

**Correspondence*: PD Dr. P. Felder
Physikalisch-Chemisches Institut
der Universität Zürich
Winterthurerstrasse 190
CH-8057 Zürich

detection. The principle of PTS is illustrated in *Fig. 1a* and can be summarized as follows. 'Parent' molecules in a collimated beam are dissociated by means of a pulsed photolysis laser and the resulting photofragments are then allowed to recoil within an evacuated chamber. Those fragments that are ejected in a specific direction reach a quadrupole mass spectrometer which is tuned to a suitably chosen mass-to-charge (*m/e*) ratio. The Time-of-Flight (TOF) distributions of the photofragments are measured by recording the ion count rate as a function of time after the dissociation laser pulse. With the known flight distance L between the photolysis region and the ionizer of the detector, the observed arrival time of a photofragment 'A' is readily converted to the corresponding velocity in the laboratory system. After subtraction of the molecular beam velocity one obtains the velocity v_A in the *barycentric* (=center-of-mass) frame of the parent molecule and, therefrom, the translational energy $E_T(A)$.

The original apparatus of *Wilson* and coworkers [14] featured a thermal-effusive molecular beam source, a pulsed laser for the photolysis, and a differentially pumped mass spectrometer for the detection of photofragments. Two drawbacks of this set-up were the short flight distance of 3–6 cm, which severely limited the kinetic energy resolution, and the fixed geometry, which restricted the fragment detection to species recoiling perpendicularly to the molecular beam. Because the dissociation products formed with a small recoil velocity are carried along the molecular beam direction and thus cannot be 'seen' by a perpendicularly oriented detector, early PTS investigations were restricted to dissociation processes with large translational energy release, *i.e.* mainly to the photoexcitation of repulsive electronic states. A substantial improvement of the experimental technique was achieved by *Lee* and coworkers [15], who built an apparatus with a highly sensitive rotatable detection system and a collimated supersonic molecular beam source. Much more recently, a third generation of PTS systems has been brought into operation [16][17]. Instead of a rotating detector these machines have a rotatable molecular beam source and a spatially fixed detector chamber. This allows the latter to be equipped with a sophisticated ultrahigh vacuum system which provides a high detection sensitivity and also permits the adoption of longer flight distances.

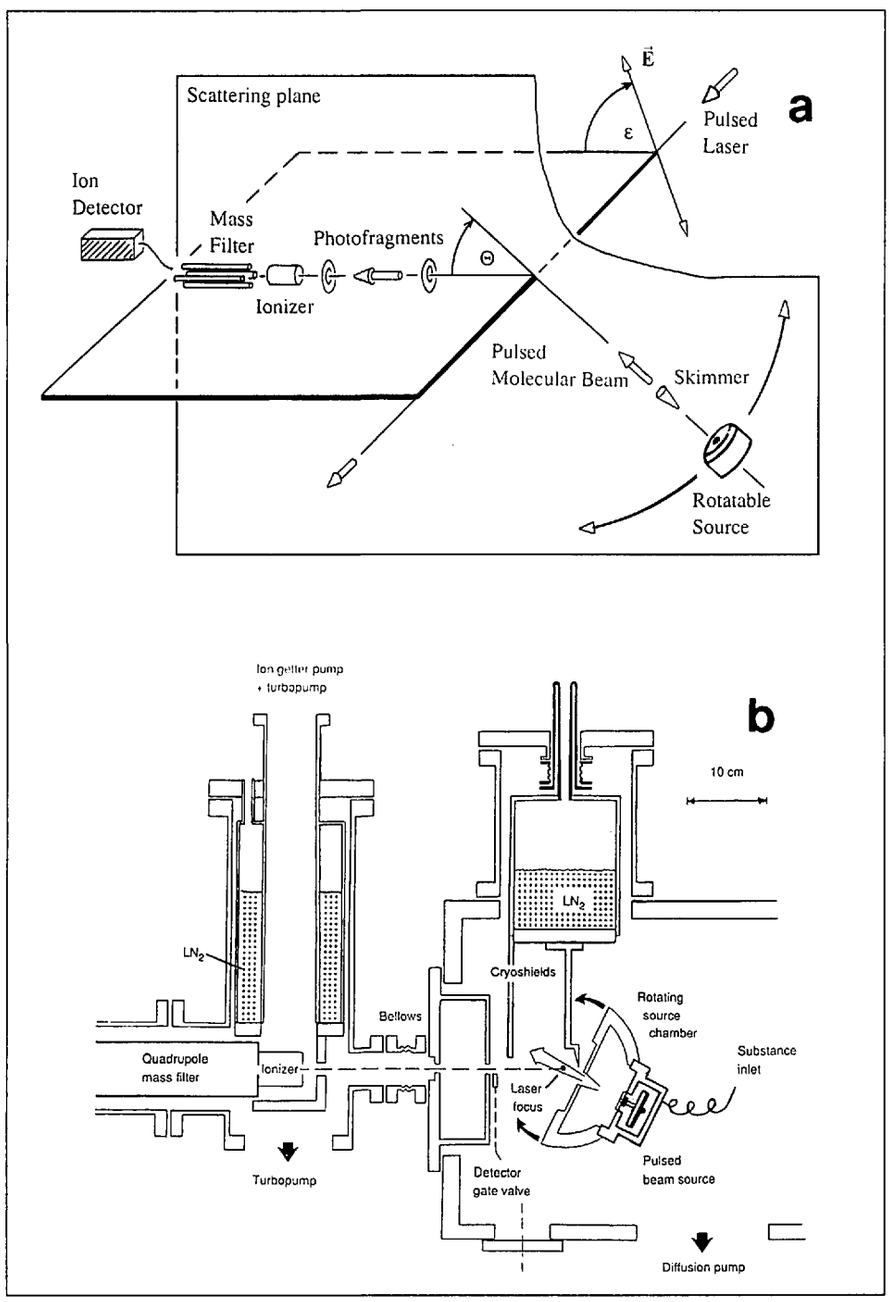

Fig. 1. a) *Principle of photofragment translational spectroscopy; b) Schematic drawing of high resolution PTS apparatus* (vertical section), *adapted from* [18]

The apparatus shown in *Fig. 1b* was designed and constructed in our laboratory [18]. It consists of a rectangular photodissociation chamber which contains a rotatable molecular beam source, and of an externally mounted detector chamber with a quadrupole mass spectrometer. A cylindrical chamber mounted inside the main chamber acts as the first differential pumping stage for the molecular beam. The latter is generated with a piezoelectrically driven valve which produces short gas pulses of *ca.* 300 μs duration and 40 Hz repetition rate. The adoption of a pulsed molecular beam source allows for a compact construction, since the low substance throughput requires only a modest pumping system. Moreover, it makes experiments with expensive compounds (*e.g.* isotopically labelled substances [19]) affordable. The pulsed supersonic jet emerging from the valve orifice is sampled with a conical skimmer which leads into the photodissociation chamber. Photodissociation is induced with a pulsed UV laser which is synchronized with the molecular beam pulse. The resulting photofragments are then detected after a flight path of 34.5 cm. With such a long flight distance, the packet of photofragments arriving at the detector has a density of typically 1000 particles/cm^3, corresponding to a partial pressure of only 4×10^{-14} mbar. To distin-

guish the weak signal of the photofragments from the overwhelming background signal caused by the residual gas in the detector, an exceedingly good vacuum system is required. This was achieved in our apparatus by means of multiple differential pumping stages (see *Fig. 1b*). The innermost detector region, which surrounds the electron impact ionizer, is pumped by a greaseless, magnetically suspended turbomolecular pump which uses another turbomolecular pump as a forepump; after extensive bakeout of the system, an operating pressure of *ca.* 8×10^{-11} mbar is attained.

While the first PTS experiments reported in the literature were carried out with frequency doubled ruby or neodymium lasers as the photolysis source, later investigations were mainly done with rare gas halide excimer lasers, since these can produce intense UV pulses (≈ 0.2 J) with a high repetition rate (≈ 100 Hz). By proper choice of the laser gas mixture, the following emission wavelengths are now routinely available: 351 nm (XeF), 308 nm (XeCl), 248 nm (KrF), 222 nm (KrCl), and 193 nm (ArF).

As an example for the application to a small molecule, we consider the photodissociation of SO_2 at 193 nm [17][19]:

$$SO_2 + h\nu \rightarrow SO + O. \qquad (1)$$

At this wavelength, the primary photofragments are formed exclusively in their electronic ground states, $SO(X^3\Sigma^-)$ and $O(^3P)$, respectively. The TOF distribution of the SO fragments (*m/e* = 48) recorded with laboratory scattering angle $\Theta = 45$ (angle between detection axis and molecular beam direction, *cf. Fig. 1a*) is displayed in *Fig. 2a*. The signal exhibits three components which are due to the formation of the SO fragment in its three lowest vibrational states, v = 0, 1, and 2. Interestingly, the TOF distribution of the O atoms (*m/e* = 16, see *Fig. 2b*) shows a very similar shape, albeit at earlier arrival times than the SO product. The similarity of the TOF spectra is a consequence of *linear momentum conservation*, which implies that in the barycentric frame the two members of a photofragment pair recoil in opposite directions and with velocities in inverse proportion of their masses, *i.e.*

$$\frac{v_O}{v_{SO}} = \frac{m_{SO}}{m_O} \qquad (2)$$

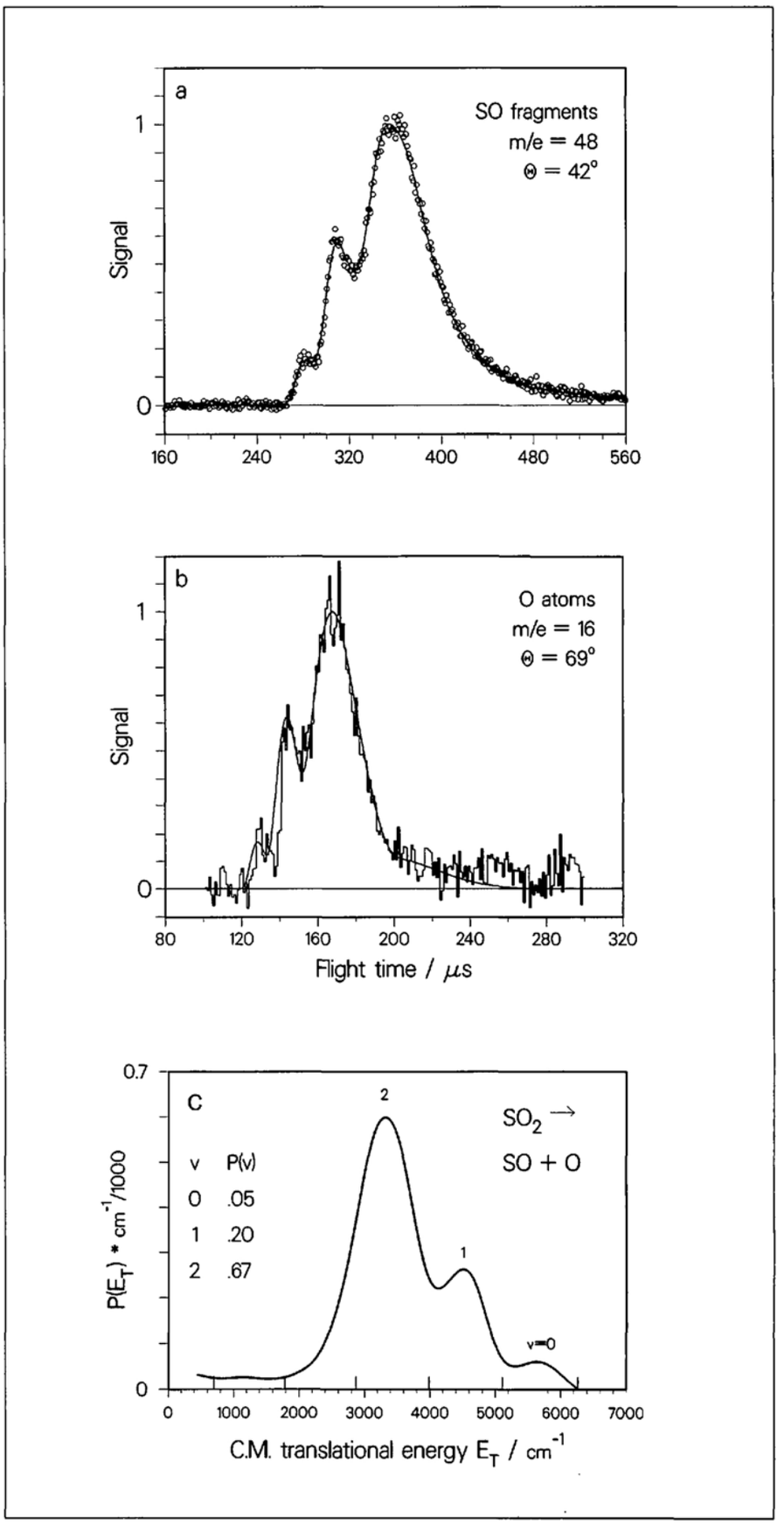

Fig. 2. *Photodissociation of SO_2 at 193 nm, adapted from* [19]. *a*) TOF distribution of the SO fragments (*m/e* = 48) with laboratory angle $\Theta = 42°$. *b*) TOF distribution of the O atoms (*m/e* = 16) with $\Theta = 69°$. *c*) Best-fitting total translational energy distribution $P(E_T)$. The solid curves in *a*) and *b*) are the best fits to the TOF data and were obtained with the energy distribution displayed in *c*).

The TOF distributions of the O-atoms and SO fragments are strictly correlated and thus contain the same information. In principle, it would suffice to measure the TOF spectrum of one fragment species, although it is advisable in practice to measure that of the counterfragment species as well. This is particularly important with larger molecules where several dissociation processes usually compete with each other (see below).

Returning to the photodissociation of SO_2, the *energy balance* can be written as

$$E_{int}(SO_2) + h\nu - D_0 = E_T(SO) + E_{int}(SO) + E_T(O) \quad (3)$$

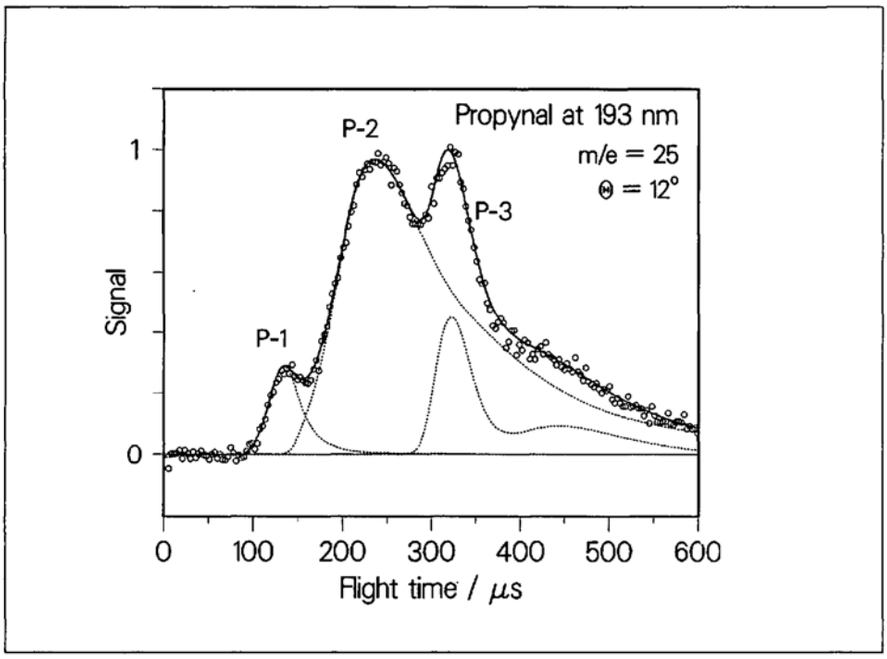

Fig. 3. *Photodissociation of propynal at 193 nm, adapted from* [29]. TOF distribution measured at $m/e = 25$ and $\Theta = 12°$. Fragments from all three primary dissociation channels are detected simultaneously as C_2H^+. These are C_2H_2 (P-1), C_2H (P-2), and HCCCO (P-3).

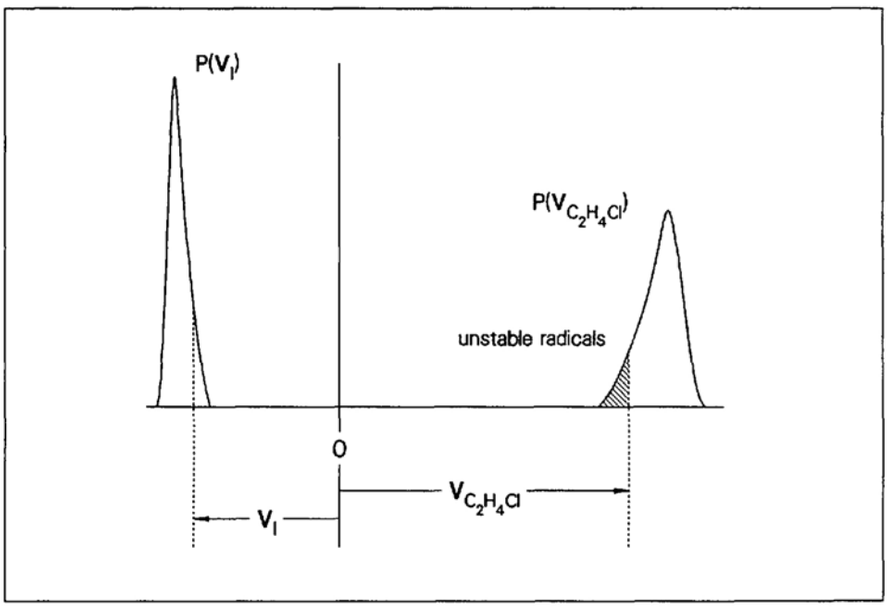

Fig. 4. *Photodissociation of 1-chloro-2-iodoethane* (CIE), *adapted from* [33]. Schematic diagram of the photofragment recoil in the CM frame of the parent molecule. Because of momentum conservation the velocity distributions of the two fragment species are strictly correlated. However, secondary dissociation causes a depletion in the TOF signal of the CH_2ClCH_2 radicals as compared to that of the I-atoms. This depletion (shaded area) occurs among the slowest, internally hottest CH_2ClCH_2 radicals.

where $h\nu$ is the photon energy, D_0 is the dissociation energy of *Reaction 1*, and E_{int} and E_T denote the internal and translational energy of a species, respectively. Because the SO_2 molecules are cooled to very low temperatures in the pulsed supersonic expansion, $E_{int}(SO_2)$ can be neglected. Moreover, since the photon energy $h\nu$ is well defined and D_0 is a constant, we introduce the available energy $E_{avl} = h\nu - D_0$ that is, the excess energy to be distributed among the product degrees of freedom. In addition, since the translational energies of SO and O are correlated, it is customary to collect them in a single term, the so-called *total translational energy* $E_T = E_T(SO) + E_T(O)$. Thus, we obtain the simple relationship

$$E_{int}(SO) = E_{avl} - E_T \quad (4)$$

which states that the total translational energy distribution $P(E_T)$ is directly related to the internal energy distribution of the SO photofragments. The best-fitting $P(E_T)$ distribution derived from the measured TOF data of SO_2 is displayed in *Fig. 2c*. It represents the probability for the formation of a fragment pair SO + O with a given total translational energy E_T, but by virtue of *Eqn. 4* it also reflects the probability for the SO fragment to possess an internal energy $E_{int}(SO) = E_{avl} - E_T$. The assignment of the three components of $P(E_T)$ to the vibrational states of the SO product is based on the close agreement between the observed energy separation of *ca.* 1100 cm^{-1} and the known vibrational energy $w_e = 1124\ cm^{-1}$ [20]. The relative areas of the components, therefore, represent the relative populations of the vibrational states of SO which, in the case at hand, deviate strongly from a thermal *Boltzmann* distribution. This non-statistical population of product states is highly specific, as we were able to show by means of isotopically labelled SO_2 [19].

Translational spectroscopy as a probe of the vibrational and electronic state distributions in nascent photofragments has been successfully applied to a number of systems and has thereby provided us with new insight into the underlying photodissociation dynamics. Among the molecules investigated at the University of Zürich, we should like to mention CF_3I [18], C_2F_4 [21], CF_2I_2 [22], ClNO [23], Cl_2SO [24] and N_2O [25].

In general, the photolysis of larger molecules gives rise to more than one primary dissociation pathway and contradictory results are found in the literature

about the identity and relative importance of various competing decay channels. For example, it has long been known that the UV photolysis of acrolein (prop-2-enal, $CH_2=CHCHO$) yields the stable products C_2H_4 and CO, but also the radical pairs C_2H_3 and HCO [26]. Due to the instability of the radicals, the branching ratio between the two processes is not easily determined under bulk conditions, where one usually has to rely on scavenging techniques and on the analysis of the stable end products. In contrast, the PTS method is ideally suited for the detection of nascent reaction products. However, the identification of the various photofragment species is rendered difficult by the cracking of the ions formed in the electron-bombardment ionizer. For instance, the methoxy radical CH_3O produced upon the photolysis of CH_3ONO [27] or CH_3OOH [28] is not detectable at the mass of its parent ion (*m/e* = 31) because of the efficient formation of daughter ions HCO^+ (*m/e* = 29). This would seem to preclude a distinction between CH_3O and, say, HCO photofragments, but fortunately the flight time of the dissociation products constitutes an additional dimension of the mass spectra. This is exemplified by the photodissociation of propynal ($CH\equiv C-CHO$) at 193 nm, which was found [29] to occur *via* three competing decay pathways (see the *Table*). The TOF distribution recorded with *m/e* = 25 (C_2H^+) displayed in *Fig. 3* shows three distinct components which have been unambiguously assigned to the photofragments species C_2H_2 from the decarbonylation process, C_2H from C–C bond fission and HCCCO from aldehydic C–H bond fission. This conclusion was reached after careful comparison of the TOF distributions obtained at several *m/e* ratios [29]. For example, the peak denoted as P-1 in *Fig. 3* is readily assigned to the acetylene product, since it coincides with the only feature observable at *m/e* = 26, where only C_2H_2 can contribute to the photofragment signal.

Similar experiments have allowed us to characterize the collision-free photochemistry of other polyatomic molecules (see the *Table*) and in some cases have shown unanticipated results: the photolysis of the sulfur ring compound thiirane proceeds mainly *via* fission of a C–H bond [30], whereas in nitric acid and methyl nitrate, the cleavage of the weak O–N bond efficiently competes with the rupture of the much stronger terminal N=O bond [31][32].

In many photochemical reactions some of the photofragments are formed with sufficient internal energy to undergo a secondary dissociation step. This 'loss' of primary photofragments causes a depletion of the corresponding TOF signal and, hence, to a deviation form the momentum correlation between the TOF distributions of the primary photoframgent pairs. Consider, *e.g.*, the photodissociations of 1-chloro-2-iodoethane (CH_2ClCH_2I) [33]. The photolysis of this molecule at 266 and 248 nm leads to the formation of I-atoms and chloroethyl radicals CH_2ClCH_2. While the C–Cl bond is rather strong in the parent molecule (*ca.* 335 kJ/mol), it is much weaker in the chloroethyl radical. As detailed in [33], depending on the electronic state of the nascent I-atom and on the amount of energy channeled into translation, the CH_2ClCH_2 radical will be either stable or unstable with respect to secondary C–Cl bond fission. From a careful comparison of the TOF distributions of the I atoms, which are not affected by the secondary dissociation, with those of the CH_2ClCH_2 radicals the fraction of the radicals that are unstable was established in a straightforward way (see *Fig. 4*). In the case at hand, the secondary decay occurs, if the internal energy exceeds 90 kJ/mol, which in turn implies that the C–Cl bond energy in the radical cannot be larger than 90 kJ/mol [34].

The determination of dissociation thresholds in free radicals mentioned above is particularly interesting, because it is based on an approach that is entirely different from other experimental methods used for this purpose. Comparison of the results thus allows one to check for systematic errors of the threshold energies. For example, using *tert*-butyl hypochlorite as a precursor molecule, we have recently investigated the unimolecular decay of the *tert*-butoxy radical [35], a species known to participate in various reactions in the troposphere [5]. We found that unimolecular dissociation to acetone and methyl radicals sets on at an internal energy of 84 kJ/mol, which is *ca.* 20 kJ/mol higher than the activation energy derived from gas kinetic rate measurements.

Finally, we address the angular distribution of the photofragments. As has first been demonstrated by *Zare* and *Herschbach* [36], the flux of the dissociation products is, in general, anisotropic. Experiments with a linearly polarized photolysis laser provide valuable information about the *symmetry* of the excited electronic states and about the time *scale* of the photodissociation process [37]. For a one-photon electric dipole transition, the photofragment angular distribution in the barycentric system is given in [36]

$$w(\upsilon) = \frac{1}{4\pi}(1 + \beta P_2(\cos\upsilon)) \qquad (5)$$

where υ is the angle between the electric vector of the laser and the recoil direction of the fragments, P_2 is the second order

Table. *Competing Primary Dissociation Processes Observed after 193-nm Photolysis of Propynal (P)* [29], *Acrolein (A)* [29], *Thiirane (T)* [30], *Nitric Acid (N)* [31], *and Methyl Nitrate (M)* [32]

Products			Relative yield	
H–C≡C–CHO	→	CH≡CH + CO	0.35	(P-1)
		CH≡C + CHO	0.30	(P-2)
	→	CH≡C–CO + H	0.35	(P-3)
H_2C=CH–CHO	→	H_2C=CH_2 + CO	[a])	(A-1)
	→	H_2C=CH + CHO	[a])	(A-2)
	→	H_2C=CH–CO + H	[a])	(A-3)
$H_2\overline{C-S-C}H_2$	→	CH_2=CH_2 + S	0.1	(T-1)
	→	CH_2=CH + HS	0.1	(T-2)
	→	CH_2–S–CH + H	0.8	(T-3)
$HONO_2$	→	OH + NO_2	0.6	(N-1)
	→	HONO + O	0.4	(N-2)
CH_3ONO_2	→	CH_3O + NO_2	0.7	(M-1)
	→	CH_3ONO + O	0.3	(M-2)

[a]) Products formed in comparable amounts.

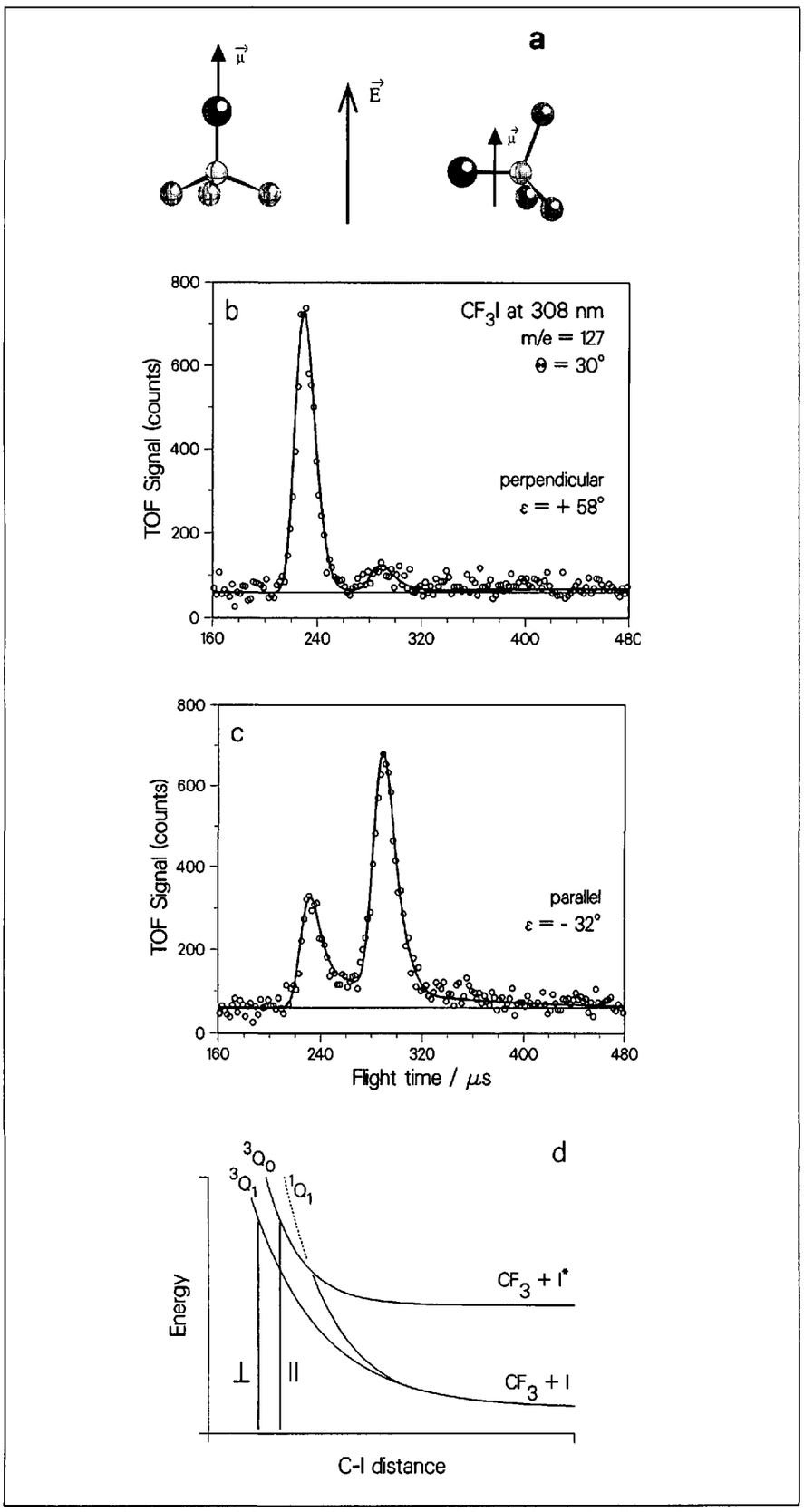

Fig. 5. *Photodissociation of CF_3I at 308 nm, adapted from* [40]. *a*) Parallel and perpendicular electronic transitions of the parent molecule lead to photofragment ejection either along the polarization direction (β=+2, left panel) or perpendicular to it (β=−1, right panel). *b*) TOF distribution of the I atoms (*m/e* = 127) with beam source angle $\Theta = 30°$ and polarization angle $\varepsilon = 58°$, which enhances the signal from fragments recoiling perpendicular to the electronic transition dipole moment. *c*) The analogous signal obtained with $\varepsilon = -32°$. *d*) Section of the pertinent potential energy surfaces of CF_3I. Photoexcitation at 308 nm gives access to the repulsive states $^3Q_1$ and $^3Q_0$ *via* perpendicular and parallel transitions, respectively.

Legendre polynomial and β is the so-called recoil anisotropy parameter. The limiting values $\beta = +2$ and -1 correspond to the distributions $\cos^2\upsilon$ and $\sin^2\upsilon$, respectively, whereas $\beta = 0$ represents an isotropic distribution. If dissociation occurs promptly after photon absorption, the value of β is determined by the *recoil geometry of the molecule*, *i.e.* by the angle χ between the electronic transition moment μ and the recoil direction:

$$\beta = P_2(\cos\chi). \qquad (6)$$

This is illustrated in *Fig. 5a* for the case of an axially symmetric molecule such as CF_3I. For symmetry reasons, the transition moment is either parallel to the C–I bond axis, in which case $\chi = 0°$ and $\beta = +2$, or it is perpendicular to it, resulting in $\chi = 90°$ and $\beta = -1$. However, if the molecule undergoes appreciable rotation before dissociating, the angular distribution will be smeared out. Hence, the deviation of β from its limiting value allows one to estimate the time scale of the dissociation process by using the parent molecule's rotation as a picosecond clock.

While these basic principles have been known for a long time, their practical applicability has steadily grown with the development of better equipment. The high sensitivity and kinetic energy resolution of our PTS apparatus have allowed us to determine, for the first time, the anisotropy parameter as *a function of kinetic energy* [23][38]. The availability of these data prompted the development of new methods for the analysis of recoil distributions [39]. The elegance of anisotropy measurements is illustrated with the photolysis of CF_3I at 308 nm [40]. *Fig. 5* shows the TOF distributions of the I atoms obtained with two mutually orthogonal polarizations of the laser. Two peaks are evident in both cases due to the formation of the two two electronic states $I(^2P_{3/2})$ and $I^*(^2P_{1/2})$. The peak at *ca.* 240 μs stems from ground state atoms and shows a perpendicular polarization ($\beta = -0.46 \pm 0.05$) whereas the peak at ≈ 300 μs arises from spin-orbit excited atoms and is polarized parallel ($\beta = +1.78 \pm 0.05$). Based on the known electronic states of CF_3I (see *Fig. 5d*) we conclude from our observations that $I^*(^2P_{1/2})$ is formed exclusively *via* the parallel transition to the state $^3Q_0$, whereas $I(^2P_{3/2})$ is formed both *via* the perpendicular transition to $^3Q_1$ and by initial excitation of $^3Q_0$ followed by a curve crossing to the $^1Q_1$ state.

In summary, we have shown that PTS can be a fruitful technique for the investi-

gation of gas-phase photodissociation processes. The universality of mass spectrometric detection combined with the rather simple principle of the PTS method have allowed us to study a variety of phenomena associated with the photodissociation of small polyatomic molecules. It is expected that PTS will continue to be an important experimental tool for the elucidation of mechanistic features of dissociation processes, particularly in the case of atmospherically relevant species [28] [31][32][35][41–43]. To this end, a recently developed metal free pulsed valve [28] makes feasible the investigation of the photolysis of corrosive species, as has been demonstrated with nitric acid [31]. Considerable efforts are also being spent on the development of molecular beam sources producing free radicals, since the photochemistry of the latter is still a poorly explored field. Finally, new laser systems providing intense and tunable UV radiation will permit detailed studies of the wavelength dependence of the dissociation dynamics and relative yield of competing decay reactions. Such results are particularly interesting with regard to a comparison with theoretical calculations based on ab *initio* potential-energy surfaces of the dissociating molecule.

Financial support of this work by the *Schweizerischer Nationalfonds zur Förderung der wissenschaftlichen Forschung* and by the *Alfred Werner Legat* is gratefully acknowledged. The author is greatly indebted to Prof. *J.R. Huber* for generous support and guidance of this work.

Received: November 19, 1993

[1] M. Shapiro, R. Bersohn, *Ann. Rev. Phys. Chem.* **1982**, *33*, 409; J.R. Huber, *Pure Appl. Chem.* **1988**, *60*, 947.

[2] R. Schinke, 'Photodissociation Dynamics', Cambridge University Press, Cambridge, 1993.

[3] M.N.R. Ashfold, J.E. Baggott, Eds., 'Molecular Photodissociation Dynamics', The Royal Society of Chemistry, London, 1987.

[4] J.R. Huber, R. Schinke, *J. Phys. Chem.* **1993**, *97*, 3463.

[5] B.J. Finlayson-Pitts, J.N. Pitts, Jr., 'Atmospheric Chemistry', Wiley, New York, 1986.

[6] R.P. Wayne, 'Chemistry of Atmospheres', Clarendon Press, Oxford, 1991.

[7] W.B. De More, S.P. Sander, D.M. Golden, M.J. Molina, R.F. Hampson, M.J. Kurylo, C.J. Howard, A.R. Ravishankara 'Chemical Kinetics and Photochemical Data for use in Stratospheric Modeling', Evaluation 9, Publication 90-1, Jet Propulsion Laboratory, Pasadena, 1990.

[8] 'Mode Selectivity in Unimolecular Reactions', *Chem. Phys.* **1989**, *139*, Special Issue.

[9] R.D. Mc Alpine, D.K. Evans, *Adv. Chem. Phys.* **1985**, *60*, 31.

[10] See *e.g. Lambda Highlights*, April 1990, 1.

[11] G.E. Hall, N. Sivakumar, P.L. Houston, I. Burak, *Phys. Rev. Lett.* **1986**, *56*, 1671; M. Dubs, U. Brühlmann, J.R. Huber, *J. Chem. Phys.* **1986**, *84*, 3106; K.-H. Gericke, S. Klee, F.J. Comes, R.N. Dixon, *J. Chem. Phys.* **1986**, *85*, 4463; M.P. Docker, A. Hodgson, J.P. Simons, *Chem. Phys. Lett.* **1986**, *128*, 264; X. Zu, B. Koplitz, C. Wittig, *J. Chem. Phys.* **1987**, *87*, 1062.

[12] J.P. Simons, *J. Phys. Chem.* **1987**, *91*, 5378; P.L. Houston, *ibid.* **1987**, *91*, 5388; G.E. Hall, P.L. Houston, *Ann. Rev. Phys. Chem.* **1989**, *40*, 375; M.P. Docker, A. Ticktin, U. Brühlmann, J.R. Huber, *J. Chem. Soc., Faraday Trans. 2* **1989**, *85*, 1169.

[13] A.H. Zewail, *Science* **1988**, *242*, 1645.

[14] G.E. Busch, J.F. Cornelius, R.T. Mahoney, R.I. Morse, D.W. Schlosser, K.R. Wilson, *Rev. Sci. Instrum.* **1970**, *41*, 1066.

[15] M.J. Coggiola, P.A. Schulz, Y.T. Lee, Y.R. Shen, *Phys. Rev. Lett.* **1977**, *38*, 17.

[16] A.M. Wodtke, Y.T. Lee, *J. Phys. Chem.* **1985**, *89*, 4744; N.P. Johnson, M.D. Barry, P.A. Gorry, *J. Phys. E: Sci. Instrum.* **1986**, *19*, 808; W.B. Tzeng, H.M. Yin, W.Y. Leung, J.Y. Luo, S. Nourbakhsh, G.D. Flesh, C.Y. Ng, *J. Chem. Phys.* **1988**, *88*, 1658.

[17] P. Felder, C.S. Effenhauser, B.-M. Haas, J.R. Huber, *Chem. Phys. Lett.* **1988**, *148*, 417.

[18] P. Felder, *Chem. Phys.* **1990**, *143*, 141.

[19] P. Felder, B.-M. Haas, J.R. Huber, *Chem. Phys. Lett.* **1993**, *204*, 248.

[20] G. Herzberg, 'Molecular Spectra and Molecular Structure I. Spectra of Diatomic Molecules', Krieger, Malabar, 1989.

[21] T.K. Minton, P. Felder, R.C. Scales, J.R. Huber, *Chem. Phys. Lett.* **1989**, *164*, 113.

[22] E.A.J. Wannenmacher, P. Felder, J.R. Huber, *J. Chem. Phys.* **1991**, *95*, 986; G. Baum, P. Felder, J.R. Huber, *ibid.* **1993**, *98*, 1999.

[23] B.-M. Haas, P. Felder, J.R. Huber, *Chem. Phys. Lett.* **1991**, *180*, 293.

[24] G. Baum, C.S. Effenhauser, P. Felder, J.R. Huber, *J. Phys. Chem.* **1992**, *96*, 756.

[25] P. Felder, B.-M. Haas, J.R. Huber, *Chem. Phys. Lett.* **1991**, *186*, 177.

[26] E.P. Gardner, P.D. Sperry, J.G. Calvert, *J. Phys. Chem.* **1987**, *91*, 1922, and ref. cit. therein.

[27] B.A. Keller, P. Felder, J.R. Huber, *J. Phys. Chem.* **1987**, *91*, 1114; P. Felder, B.A. Keller, J.R. Huber, *Z. Phys. D* **1987**, *6*, 185.

[28] M.-A. Thelen, P. Felder, J.R. Huber, *Chem. Phys. Lett.* **1993**, *213*, 275.

[29] B.-M. Haas, T.K. Minton, P. Felder, J.R. Huber, *J. Phys. Chem.* **1991**, *95*, 5149.

[30] P. Felder, E.A.J. Wannenmacher, I. Wiedmer, J.R. Huber, *J. Phys. Chem.* **1992**, *96*, 4470.

[31] P. Felder, X. Yang, J.R. Huber, *Chem. Phys. Lett.*, in press.

[32] X. Yang, P. Felder, J.R. Huber, *J. Phys. Chem.* **1993**, *97*, 10903.

[33] T.K. Minton, P. Felder, R.J. Brudzynski, Y.T. Lee, *J. Chem. Phys.* **1984**, *81*, 1759.

[34] Under collisionless conditions, the photofragments are either stable or, if their internal energy is above threshold, decay on a time scale of nanoseconds or less. This time scale should be distinguished from that of the decomposition kinetics in the bulk phase, where collisions redistribute the energy among the molecules of the ensemble.

[35] M.-A. Thelen, P. Felder, J.G. Frey, J.R. Huber, *J. Phys. Chem.* **1993**, *97*, 6220.

[36] R.N. Zare, D.R. Herschbach, *Proc. IEEE* **1963**, *51*, 173; R.N. Zare, *Mol. Photochem.* **1972**, *4*, 1.

[37] R. Bersohn, S.H. Lin, *Adv. Chem. Phys.* **1969**, *16*, 67; C. Jonah, *J. Chem. Phys.* **1971**, *55*, 1915; G.E. Busch, K.R. Wilson, *ibid.* **1972**, *56*, 3638, S. Yang, R. Bersohn, *ibid.* **1974**, *61*, 4400.

[38] P. Felder, *Chem. Phys.* **1991**, *155*, 435.

[39] J.G. Frey, P. Felder, *Mol. Phys.* **1992**, *75*, 1419.

[40] P. Felder, *Chem. Phys. Lett.* **1992**, *197*, 425.

[41] G. Baum, J.R. Huber, *Chem. Phys. Lett.* **1993**, *203*, 261.

[42] P. Felder, C. Demuth, *Chem. Phys. Lett.* **1993**, *208*, 21.

[43] G. Baum, J.R. Huber, *Chem. Phys. Lett.* **1993**, *213*, 427.